ISBN: 978-3-95450-247-9 ISSN: 2673-5490 doi: 10.18429/JACoW-IPAC2024-MOPC04

STUDY OF ORBITAL EFFECTS ON EIC DETECTOR SYNCHROTRON RADIATION BACKGROUND

C. Liu*, C. Hetzel, A. Drees, C. Montag, Brookhaven National Lab, Upton, NY, USA.
M. Sullivan, SLAC, Menlo Park, CA, USA.

Abstract

Synchrotron radiation could contribute to detector background significantly, especially when the electron beam deviates from the design orbit. Without effective control, synchrotron radiation could impede physics data taking or even damage detector components. One of the key contributors to suppress synchrotron radiation in the Electron-Ion Collider IR is to control the electron orbit upstream the detectors. Therefore, it is imperative to define the tolerance of orbit errors in the IR which requires studying the orbital effects on synchrotron radiation. In this report, we will present the studies of orbital effects on synchrotron radiation background in EIC IR, including beam offsets introduced by upstream dipole, correctors, and quadrupole offsets.

INTRODUCTION OF THE EIC AND THE MOTIVATION OF THE SYNCHROTRON RADIATION STUDY

The Electron-Ion Collider (EIC) is a forthcoming particle accelerator designed for colliding electrons with protons and nuclei to delve into their internal structures [1, 2]. This collider will be constructed jointly by the Brookhaven National Lab (BNL) and the Thomas Jefferson National Accelerator Facility. Alongside upgrading the Relativistic Heavy Ion Collider facility, electron sources and accelerators will be installed in the existing tunnel to provide electrons at energy levels of 5, 10, and 18 GeV for collision experiments. The electrons in the Electron Storage Ring (ESR) [3] will be colliding with the hadrons in the Hadron Storage Ring (HSR) at 25 mrad crossing angle in the EPIC experimental area.

Synchrotron radiation originating from the electron beam upstream of the detector poses a notable background concern. Efforts were made in design to mitigate this impact, including the placement of a weak dipole ahead of the detector and the addition of a scraper to partially attenuate the radiation. Nevertheless, synchrotron radiation remains a concern due to potential deviations in the electron orbit from the design trajectory. Moreover, upstream dipole correctors and quadrupoles could introduce additional radiation sources.

To address these challenges, an orbit correction system is imperative to rectify orbit deviations caused by machine errors, especially in the Electron Storage Ring (ESR) and the Infrared (IR) region. This paper aims to explore key questions: How might anticipated machine errors and required corrections, such as dipole kicks, impact the characteristics of synchrotron radiation in the IR? And to what extent might this affect the intensity of synchrotron radiation on the detector beam pipe?

INTRODUCTION TO THE ESR ORBIT CORRECTION

The author's objective was to develop the ESR orbit correction system and assess its effectiveness in controlling the orbit, particularly in the IR region of the ring. Following the HERA-e scheme, correctors and BPMs were strategically placed in the ESR, with dual-plane BPMs situated at defocusing quadrupoles and horizontal/vertical correctors positioned at focusing/defocusing quadrupoles.

Table 1 shows the machine errors included in the ESR for evaluating the orbit deviation and orbit correction scheme.

Table 1: Machine Errors Included in ESR for Orbit Study

Errors	Value	Note
Quad Misalignment	50 μm	rms
BPM Misalignment	50 μm	rms
Quad Gradient	10^{-4}	relative
Quad Roll	0.5 deg	rms
BPM Resolution	±20 μm	peak-to-peak
Dipole Corrector	0.2×10^{-3}	rms

Figure 1 shows the ESR horizontal orbit with machine errors in blue, and the orbit after engaging the orbit correction in orange. The orbit in the vertical plane shows the same effect but not shown here.

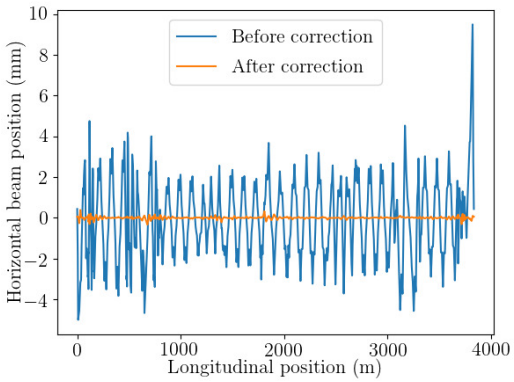

Figure 1: The ESR horizontal orbit distortion with machine errors and the orbit after correction.

In the following studies, we will narrow down to the region ± 100 m around the IP [4] for orbit and synchrotron radiation

* cliu1@bnl.gov; Work supported by Brookhaven Science Associates, LLC under Contract No. DE-AC02-98CH10886 with the U.S. Department of Energy.

ISBN: 978-3-95450-247-9 ISSN: 2673-5490 doi: 10.18429/JACoW-IPAC2024-MOPC04

study. The actual orbit that will be studied is expected to be less optimal than the one described above, as this approach allows for a margin of tolerance to accommodate potential variations or uncertainties.

SYNRAD+ OVERVIEW AND ITS APPLICATION IN THE STUDY

SynRad+ [5] employs photon tracing techniques to compute the flux and power distribution on a surface due to synchrotron radiation. It incorporates beam orbit, envelope, and magnetic element data from the lattice file, along with beam aperture details.

Madx was utilized to produce the orbit, beam envelope functions, and lattice data. OpticsBuilder, another tool, was employed to extract inputs from Madx and create 3D geometries and magnetic regions needed for SynRad+. This process involves translating a list of beam elements and aperture specifications from an accelerator into inputs suitable for SynRad+.

Figure 2 shows the ESR IR aperture imported to SynRad+ application and Figure 3 shows the beta functions in the IR region.

Figure 2: The ESR IR aperture profile as shown in the SynRad+ application.

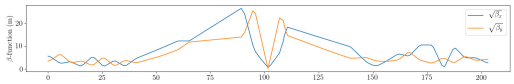

Figure 3: Beta functions in the IR region.

THE RESULTS OF SYNCHROTRON RADIATION STUDY

Beam tails in both planes were implemented with the assumption that the distributions are Gaussian. The current of the tails were set as 10% of the total beam current. The horizontal emittance of the tail is 9.2 times of the beam core emittance, while the vertical emittance of the tail is 34 times of the beam core emittance. More realistic beam tail distribution can be derived from beam-gas interaction simulation of the ESR beam for future studies.

Solenoid field map was not imported in SynRad+, however the effect will be analyzed in the last section of this paper.

As a test of the procedure, the following four cases were studied: ± 2 mm initial orbit offset, and ± 0.1 mrad initial orbit angle at ~ 100 m upstream of the IR region (shown in Figure 4). The IR region has no other errors except for the initial orbit/angle offsets. For these four cases, the primary beam does not generate any synchrotron radiation that reaches the detector beampipe.

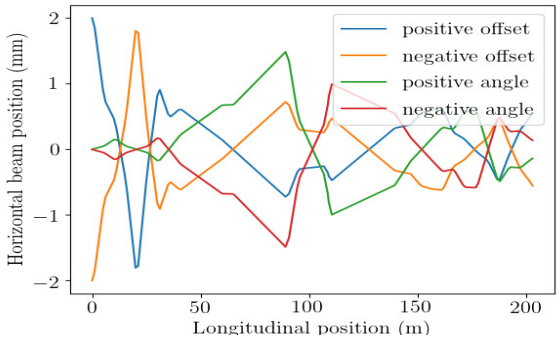

Figure 4: Horizontal orbits of the four cases studied for the synchrotron radiation.

Effect of Realistic Orbit and Quadrupole Offsets

To study cases with errors and correction stronger than one expects, the quadrupole offsets were set to be 120 µm (rms) in horizontal, 150 µm in vertical, compared to 50 µm used in ESR orbit correction simulation. In addition, there is only one iteration of orbit correction, so the residual orbit, shown in Figure 5, was not as good as the one shown in the previous section.

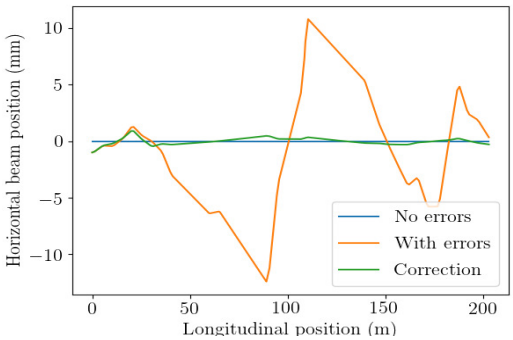

Figure 5: IR horizontal orbits for three cases: without errors in blue, with errors in orange and after correction in green.

The upstream quadrupole Q0EF (1.2 m, -12.98 T/m) was chosen to study the effect of quadrupole offsets. In addition to the previously assigned machine errors, we introduced +/- 1 mm misalignment errors to Q0EF in both planes.

In the following, we will analyze simulation outcomes across five scenarios:

1. Case 1: No errors.
2. Case 2: With errors but without correction.
3. Case 3: With errors with correction.
4. Case 4: With errors, positive Q0EF offset, and correction.
5. Case 5: With errors, negative Q0EF offset, and correction.

ISBN: 978-3-95450-247-9 ISSN: 2673-5490 doi: 10.18429/JACoW-IPAC2024-MOPC04

The radiation power levels at the detector beam pipe and a mask, located 3.6 meters upstream of the interaction point (IP), are illustrated below.

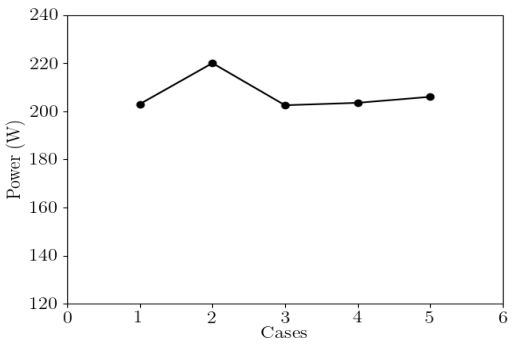

Figure 6: Synchrotron radiation power produced on the mask by the primary beam for the five study cases.

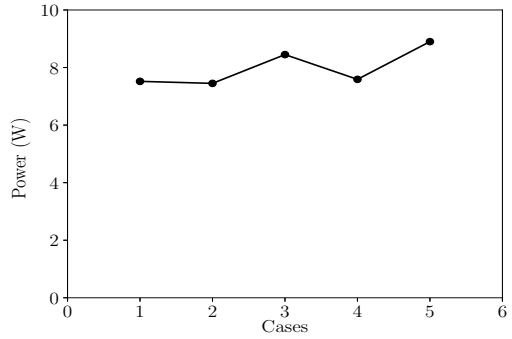

Figure 7: Synchrotron radiation power produced on the detector beampipe by the primary beam for the five study cases.

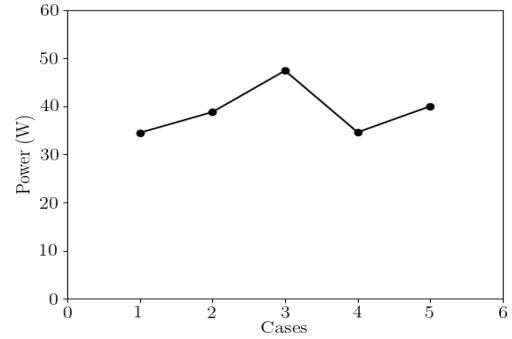

Figure 8: Synchrotron radiation power produced on the mask generated by the tail beam for the five study cases.

As shown in the Figures 6–9, the mask is intercepting most of the power generated by the primary and the tail beam. The orbit distortion could lead to approximately 20% higher synchrotron radiation levels at the mask, although

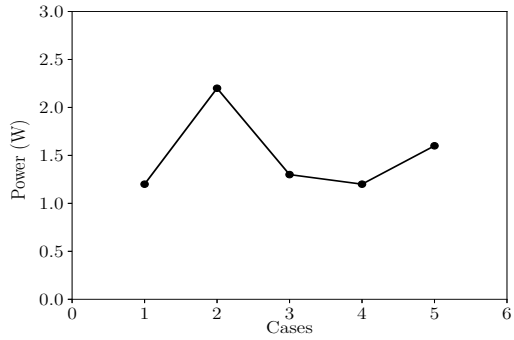

Figure 9: Synchrotron radiation power produced on the detector beampipe by the tail beam for the five study cases.

this effect is not observed on the detector beampipe. Additionally, a quadrupole offset of about ±1 mm does not result in significant changes in synchrotron radiation levels on the detector beampipe. The effect of synchrotron radiation of several Watts on the detector beampipe is yet to be simulated.

EFFECT OF THE EXPERIMENTAL SOLENOID

Figure 10 shows the distribution of the experimental solenoid longitudinal field. The effect of the experimental solenoid will be evaluated in the following.

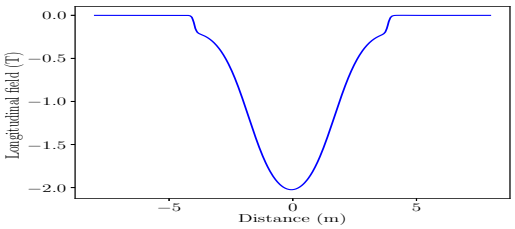

Figure 10: Distribution of the experimental solenoid longitudinal field.

The electron beam experience edge focusing of the experimental solenoid and go on Larmor motion inside the solenoid body. The focusing is measured in focal length $f = \frac{4(B\rho)^2}{\int B^2 ds} = 1200$ m, which is significantly weaker than any ESR quads.

Assuming the orbit at the two BPMs near IP6 can be controlled within $\pm$ 2 mm, the beam incident angle θ is about $\pm$ 0.2 mrad. The bending field in the transverse plane in the solenoid is $B_z * \theta = 4 * 10^{-4}$ (T). Hence, neither the edge focusing nor the body field is sufficiently strong to generate observable synchrotron radiation.

REFERENCES

[1] F. Willeke and J. Beebe-Wang, "Electron Ion Collider Conceptual Design Report 2021,"Office of Scientific and Technical Information (OSTI), Feb. 2021. doi:10.2172/1765663.

ISBN: 978-3-95450-247-9 ISSN: 2673-5490 doi: 10.18429/JACoW-IPAC2024-MOPC04

[2] C. Montag *et al.*, "The EIC accelerator: design highlights and project status", presented at the IPAC'24, Nashville, TN, USA, May 2024, paper MOPC67, this conference.

[3] D. Marx *et al.*, "Design Updates to the EIC Electron Storage Ring Lattice", presented at the IPAC'24, Nashville, TN, USA, May 2024, paper MOPC73, this conference.

[4] H. Witte *et al.*, "Progress on the design of the interaction region of the Electron-Ion Collider EIC", presented at the IPAC'24, Nashville, TN, USA, May 2024, paper MOPC75, this conference.

[5] K. Roberto and A. Marton, "Recent developments of Monte-Carlo codes Molflow+ and Synrad+", CERN, Geneva, Switzerland, CERN-ACC-2019-173, 2019.